articles

molecular pharmaceutics

Biodistribution and Pharmacokinetic Analysis of Paclitaxel and Ceramide Administered in Multifunctional Polymer-Blend Nanoparticles in Drug Resistant Breast Cancer Model

Lilian E. van Vlerken,[†] Zhenfeng Duan,[‡] Steven R. Little,[§] Michael V. Seiden,[||] and Mansoor M. Amiji*,[†]

Department of Pharmaceutical Sciences, Northeastern University, Boston, Massachusetts, Department of Orthopedic Surgery, Massachusetts General Hospital, Boston, Massachusetts, Department of Chemical Engineering, University of Pittsburgh, Pittsburgh, Pennsylvania, and Fox Chase Cancer Center, Philadelphia, Pennsylvania

Received February 27, 2008; Revised Manuscript Received June 16, 2008; Accepted June 18, 2008

Abstract: In this study, we have investigated the biodistribution and pharmacokinetic analysis of paclitaxel (PTX) and the apoptotic signaling molecule, C_6-ceramide (CER), when administered in a multifunctional polymer-blend nanoparticle formulation to female nude mice bearing an orthotopic drug sensitive MCF7 and multidrug resistant $MCF7_{TR}$ (*MDR-1* positive) human breast adenocarcinoma. A polymer-blend nanoparticle system was engineered to incorporate temporally controlled sequential release of the combination drug payload. Hereby, PTX was encapsulated in the pH-responsive rapid releasing polymer, poly(beta-amino ester) (PbAE), while CER was present in the slow releasing polymer, poly(D,L-lactide-*co*-glycolide) (PLGA) within these blend nanoparticles. When particle formulations were administered intravenously to MCF7 and $MCF7_{TR}$ tumor bearing mice, higher concentrations of PTX were found in the blood due to longer retention time and an enhanced tumor accumulation relative to administration of free drug. In addition, the PLGA/PbAE blend nanoparticles were effective in enhancing the residence time of both drugs at the tumor site by reducing systemic clearance. Overall, these results are highly encouraging for development of multifunctional polymer-blend nanoparticle formulations that can be used for temporal-controlled administration of two drugs from a single formulation.

Keywords: Multidrug resistant tumors; polymer-blend nanoparticles; paclitaxel; ceramide; biodistribution; noncompartmental pharmacokinetics

Introduction

A major clinical obstacle in cancer therapy is the development of resistance to a multitude of chemotherapeutic agents, a phenomenon termed multidrug resistance (MDR).[1] The development of drug resistance in a small subset of tumor cells is believed to be the cause for tumor survival despite invasive chemotherapy. Chemoresistance can generally result from either of two means: (1) by physically impairing delivery to the tumor[2] (e.g., poor absorption, increased metabolism/excretion, and/or poor diffusion of drugs into the tumor mass) or (2) through intracellular mechanisms that raise the threshold for cell death.[3–5] The latter is commonly

* Corresponding author. Mailing address: Northeastern University, Pharmaceutical Sciences Department, 110 Mugar Life Sciences Building, 360 Huntington Avenue, Boston, MA 02115. Tel: 617-373-3137. Fax: 617-373-8886. E-mail: m.amiji@neu.edu.
[†] Northeastern University.
[‡] Massachusetts General Hospital.
[§] University of Pittsburgh.
[||] Fox Chase Cancer Center.

(1) Harris, A. L.; Hochhauser, D. *Acta Oncol.* **1992**, *31* (2), 205–213.
(2) Galmarini, C. M.; Galmarini, F. C. *Curr. Opin. Invest. Drug* **2003**, *4* (12), 1415–1421.
(3) Gottesman, M. M.; Fojo, T.; Bates, S. E. *Nat. Rev. Cancer* **2002**, *2*, 48–58.
(4) Kellen, J. A. *J. Exp. Ther. Oncol.* **2003**, *3*, 5–13.

10.1021/mp800030k CCC: $40.75
Published on Web 07/11/2008

implicated in the development of MDR, and, often, more than one mechanism, either simultaneous or sequential, may be responsible for the MDR phenotype.[1,4] The most frequently occurring causes of MDR include overexpression of membrane-bound ATP-dependent drug efflux pumps from the ABC transporter family (most notably P-glycoprotein/*MDR-1*), modifications in drug metabolism through glutathione-*S*-transferase or cytochrome P450 activity, alterations in DNA repair mechanisms, and critical alterations in the cellular apoptotic signaling mechanisms.[1,3,5]

For this purpose, we have hypothesized that a multifunctional nanoparticle-based therapeutic strategy would be beneficial for the treatment of MDR tumor, especially with the use of combination strategies that evade efflux transport and lower the tumor apoptotic threshold.[6,7] Based on the principle that MDR has been shown to result from metabolism of the apoptotic mediator ceramide by the enzyme glucosylceramide synthase (GCS) to elevate the apoptotic threshold,[8–11] this novel therapeutic strategy aims to restore the alternation in the cellular apoptotic signaling through a combination therapy of paclitaxel (PTX), a microtubule stabilizing agent and promoter of apoptosis, and exogenous C_6-ceramide (CER), which can propagate apoptotic signaling and allow for enhanced cell-kill response.

Based on preliminary evidence, it was found that a combination therapy of PTX with CER is most effective against MDR breast and ovarian cancer when CER is administered with a time delay (typically 6 h) following PTX administration. To incorporate this temporal spacing of drug release, a polymer-blend nanoparticle was designed by blending 70% by weight poly(D,L-lactic-*co*-glycolic acid) (PLGA) to 30% by weight poly(beta-amino ester) (PbAE) to control release of the PTX + CER combination therapy for optimal therapeutic efficacy. This strategy was conceived based on earlier work of Little et al.,[12] where PLGA/PbAE blend microspheres were used for DNA vaccine delivery in antigen presenting cells. A large library (>5,000) of poly(beta-amino esters) (PbAEs) has been synthesized and evaluated for cellular toxicity and transfection potential, by reacting diol-diacrylates with various types of primary and secondary amines.[13,14] A representative hydrophobic PbAE, synthesized by the addition reaction of 4,4′-trimethyldipiperidine with 1,4-butanediol diacrylate, has unique pH-solubility properties; the polymer remains intact at pH 7.4, but rapidly dissolves at pH 6.5.[13] This PLGA/PbAE blend nanoparticle was designed to immediately release PTX by rapid dissolution of PbAE in a lower pH environment, such as the tumor microenvironment (pH < 6.5), or in the endosome/lysosome of a cell following internalization. Conversely, CER was expected to exhibit slower release (being localized with the pH-insensitive polymer, PLGA), facilitating cellular apoptosis. From previous studies, we have observed that the exogenously administered CER reinstates the apoptotic signal to resensitize the cancer cells to the chemotherapeutic drug PTX.[6] Additionally, long-circulating, nanoparticle-based, systemic delivery of the combination therapy enhances efficacy at the cellular level by increasing intracellular drug accumulation and optimizing the dose administered, and on a whole body level by increasing targeting and residence time of the drug at the tumor mass upon systemic administration.[15–17]

Site-specific drug delivery systems increase the therapeutic benefit by delivering a greater fraction of the dose at the target site, which minimizes the amount of therapeutic that accumulates at nonspecific targets. Drug delivery throughout the tumor mass is crucial for the treatment to be effective, since residual cancer cell survival can promote regrowth and often becomes the cause for drug resistance.[18] For colloidal carriers, such as liposomes and polymeric nanoparticles, these barriers can be overcome through the unique properties of tumor neovasculature.[19] Angiogenesis (the formation of new vasculature) associated with rapid growth of the tumor mass results in fenestrations in tumor capillaries.[20] These fenestrations (or gaps between adjacent endothelial cells), are sized around 200−400 nm.[20] In addition, the lymphatic system, which usually runs alongside the blood circulation to clear macromolecules from tissues, is impaired in solid tumors. This lack of lymphatic drainage results in decreased clearance of macromolecules (>40 kDa) within the vicinity of the tumor.[20] Together, these two physiologic parameters of the tumor mass, termed the enhanced permeability and retention

(5) Bradley, G.; Juranka, P. F.; Ling, V. *Biochem. Biophys. Acta* **1988**, *948*, 87–128.
(6) van Vlerken, L. E.; Duan, Z.; Seiden, M. V.; Amiji, M. M. *Cancer Res.* **2007**, *67* (10), 4843–4850.
(7) Devalapally, H.; Duan, Z.; Seiden, M. V.; Amiji, M. M. *Int. J. Cancer* **2007**, *121*, 1830–1838.
(8) Bleicher, R. J.; Cabot, M. C. *Biochem. Biophys. Acta* **2002**, *1585*, 172–178.
(9) Cabot, M. C.; Giuliano, A. E.; Volner, A.; Han, T.-Y. *FEBS Lett.* **1996**, *394*, 129–131.
(10) Lavie, Y.; Cao, H.; Bursten, S. L.; Giuliano, A. E.; Cabot, M. C. *J. Biol. Chem.* **1996**, *271* (32), 19530–19536.
(11) Lavie, Y.; Cao, H.; Volner, A.; Lucci, A.; Han, T. Y.; Geffen, V.; Giuliano, A. E.; Cabot, M. C. *J. Biol. Chem.* **1997**, *272* (3), 1682–1687.
(12) Little, S.; Lynn, D. M.; Ge, Q.; Anderson, D. G.; Puram, S. V.; Chen, J.; Elsen, H. N.; Langer, R. *Proc. Natl. Acad. Sci. U.S.A.* **2004**, *101* (26), 9534–9539.
(13) Lynn, D. M.; Amiji, M. M.; Langer, R. *Angew. Chem., Int. Ed.* **2001**, *40*, 1707–1710.
(14) Anderson, D. G.; Akinc, A.; Hossain, N.; Langer, R. *Mol. Ther.* **2005**, *11* (3), 426–434.
(15) Devalapally, H.; Shenoy, D.; Little, S.; Langer, R.; Amiji, M. *Cancer Chemother. Pharmacol.* **2006**(epub).
(16) Shenoy, D.; Little, S.; Langer, R.; Amiji, M. *Pharm. Res.* **2005**, *22* (12), 2107–2114.
(17) Shenoy, D. B.; Amiji, M. M. *Int. J. Pharm.* **2005**, *293*, 261–270.
(18) Bast, R. C.; Kufe, D. W.; Pollock, R. E.; Weichselbaum, R. R.; Holland, J. F.; Frei, E.; Gansler, T. S. *Cancer Medicine*, 5th ed.; American Cancer Society and BC Decker Publishing: Hamilton, Ontario, 2000.
(19) Ferrari, M. *Nat. Rev. Cancer* **2005**, *5*, 161–171.
(20) Maeda, H.; Wu, J.; Sawa, T.; Matsumura, Y.; Hori, K. *J. Controlled Release* **2000**, *65* (1−2), 271–284.

(EPR) effect,[20] can be taken advantage of to improve drug delivery to tumors mediated by nanocarriers.

Previous studies from our group have shown that paclitaxel (PTX)-containing PEO-PCL nanoparticles remain stable *in vivo*, and retain the PEO copolymer (Pluronic) surface layer to increase the circulating half-life and plasma residence time of PTX from a fraction of an hour to 25.3 and 24.0 h, respectively, alongside a nearly 8-fold decrease in total body clearance of the drug.[16,21] The concentration of PTX inside the tumor mass of mice-bearing human ovarian carcinoma (SKOV3) xenografts, as a result, was 8.7-fold higher 5 h postinjection as compared to mice treated with paclitaxel solution,[16] resulting in enhanced therapeutic efficacy of the nanoparticle formulation over solution PTX, seen by the 63% reduction of final tumor volume.[15]

To examine the effectiveness of PEO-modified PLGA/PbAE blend nanoparticles for improving the tumor accumulation of the PTX + CER drug load, as a means toward enhanced efficacy, we have administered the control and test formulations to mice bearing drug sensitive (MCF7) and MDR ($MCF7_{TR}$) human breast tumor xenografts. In this study, we have examined the biodistribution and pharmacokinetics of PTX and CER upon administration in PLGA/PbAE blend nanoparticle formulations in an orthotopic wild-type (drug sensitive) and drug resistant (*MDR-1* positive) MCF7 estrogen-positive human breast adenocarcinoma model. While it is known that nanoparticles enhance drug delivery to tumors by the EPR effect, it is unknown whether MDR physiology has any further effect on tumor drug disposition and retention. These studies, therefore, can allow for an interpretation of the effect of cellular mechanisms of MDR on tumor targeting of the drugs with blend nanoparticles.

Materials and Methods

1. Preparation and Characterization of Nanoparticle Formulations. Polymer-blend nanoparticles were manufactured by blending PLGA (MW 12 kDa, 50:50 molar ratio of lactide to glycolide) (Birmingham Polymers, Pelham, AL) with PbAE [MW 10 kDa kindly supplied by S.L. (University of Pittsburgh, Pittsburgh, PA)], in a weight ratio of 70%:30%, respectively, using solvent displacement. PTX was loaded at 2.5% (w/w) and CER at 10% (w/w) in the blend nanoparticles. In addition, the nanoparticles were coloaded with 20 μCi of ^{3}H-PTX per mg of regular PTX and 2.5 μCi of ^{14}C-CER per mg of regular CER. The radiolabeled derivatives of PTX and CER were purchased from American Radiolabeled Chemicals (St. Louis, MO).

Furthermore, for *in vivo* imaging studies, 20 μg of rhodamine-PTX per mg of regular PTX was also coloaded into the nanoparticles. PCL or PLGA was dissolved in acetone together with 20% (w/w) Pluronic F-108 and CER, while PbAE was dissolved in ethanol together with PTX. Both preparations were heated at 37 °C to facilitate dissolution, after which they were joined and instantaneously added to 10 volumes of water at pH 8.0 with rapid magnetic stirring at a rate of 2 mL/min. Polymer−drug complexes were dissolved in their respective organic phases at 10 mg of total nanoparticle mass/0.5 mL of organic solvent, using equal amounts of acetone and ethanol. Following overnight stirring to allow for evaporation of the organic solvents, nanoparticles were collected by centrifugation at 10,000 rpm for 40 min at 4 °C, washed with deionized distilled water adjusted to pH 8.0, and stored wet at 4 °C. Alongside, free drug formulations using Cremophore EL and ethanol were prepared, with similar addition of 20 μCi of ^{3}H-PTX per mg of regular (cold) PTX, 2.5 μCi of ^{14}C-CER per mg of regular CER, and 20 μg of rhodamine-PTX per mg of regular PTX. Thus, hereby, for each dose administered, the animals received radioactive tracers of 1 μCi of ^{3}H-PTX and 0.5 μCi of ^{14}C-CER, and a fluorescent tracer of 1 μg of rhodamine-PTX.

Nanoparticles were characterized for size and zeta-potential on a Brookhaven Zeta-PALS analyzer that combines dynamic light scattering for size approximation with zeta-potential analysis (Brookhaven instruments Inc., Holtsville, NY). To determine a drug release profile for PTX and CER from the nanoparticles, 10 mg of lyophilized drug-loaded nanoparticles were initially resuspended in 5 mL of PBS at pH 7.4 and incubated at 37 °C for 6 h with constant agitation. Every hour, nanoparticles were centrifuged at 10,000 rpm for 10 min, and 4 mL of release media was removed for analysis and replaced with 4 mL of PBS pH 7.4 to maintain sink conditions. At the 6 h time point, the pH of the release medium was spiked to 6.5 with HCl, after which the particles continued to incubate under constant agitation. Again, 4 mL samples of release media were removed at every hour, only now replaced with PBS at pH 6.5, and the particles were left to incubate for up until 12 h after the start of the study. PTX loading yield and subsequent release were determined by quantitating the amount of PTX by reverse-phase HPLC on a C18 column using 50% acetonitrile:50% phosphate buffer with 20 mM SDS as the mobile phase. To quantitatively track CER, a fluorescent derivative of CER, namely NBD-CER (Invitrogen Corporation, Carlsbad, CA), was loaded into the nanoparticle formulation at 1% w/w, thereby allowing for quantitation as loading yield and subsequent release by fluorescent absorption using 485 nm excitation and 535 nm emission. Studies were repeated thrice.

2. *In Vitro* Drug Efficacy Studies. Human breast adenocarcinoma (MCF7) cells and their multidrug resistant subculture $MCF7_{TR}$ were kindly provided by M.V.S. (Fox Chase Cancer Center, Philadelphia, PA) and Z.D. (Massachusetts General Hospital, Boston, MA). The $MCF7_{TR}$ subculture had been established by successive selection from exposure to increasing concentrations of paclitaxel, and was found to be at least 10-fold resistant to paclitaxel over the drug sensitive (MCF7) culture. To examine the effect of temporal spacing between administration of PTX and CER on efficacy against MDR, the MDR cells were plated at 10,000 cells per well in 96 well plates and treated with 1 μM PTX alone or alongside 10 μM CER as free drugs in solution, whereby

(21) Shenoy, D. B.; Amiji, M. M. *Int. J. Pharm.* **2005**, *293*, 261–270.

either the cotreatment was administered together, PTX was administered with a 6 h delay following CER, or CER was administered with a 6 h delay following PTX. Since PTX is a cell-cycle specific cytotoxic agent, the treatment was left to proceed for 5 days to ensure that all cells underwent mitosis. Following this incubation period, cell kill efficacy was measured by the MTS assay (Promega Corp., Madison, WI). Treatment with cell culture media was used as a negative control (0% cell death), while treatment with 100 μg/mL poly(ethyleneimine) was used as a positive control (100% cell death).

3. *In Vivo* Biodistribution and Pharmacokinetic Studies. (a) Animal Model. Female *nu/nu* (athymic) mice (Charles River Laboratories, Wilmington, MA) were housed in sterile cages with *ad libitum* access to sterile food and acidified water on a 12:12 light:dark cycle. All experiments were approved by the Institutional Animal Care and Use Committee, the Radiation Safety Committee, and the Office of Environmental Health and Safety of Northeastern University.

In order to establish and maintain MCF7 estrogen-responsive tumor *in vivo*, estradiol-containing silastic implants were surgically inserted along the right flank of mice that would receive either wild-type (MCF7) or drug resistant ($MCF7_{TR}$) tumor xenografts. For this procedure, mice were anesthetized by inhalation of a 40% isoflurane solution in USP quality mineral oil by the open drop method, and kept under anesthesia through a nose cone apparatus that administered a 30% isoflurane solution in mineral oil. A 5.0 mm incision was made between the scapula, and the subcutaneous implant was inserted longitudinally. The incision was then closed with 4-0 nylon sutures, and animals were allowed to rest and recover for at least 48 h.

(b) Orthotopic Tumor Model Development. To inoculate MCF7 or $MCF7_{TR}$ cells into the mammary fat pad for orthotopic tumor development, cultured cells were harvested and counted. For each mouse, 2×10^6 cells were resuspended into 100 μL of serum supplemented RPMI, to which 100 μL of Matrigel HC (BD Biosciences, San Jose, CA) was mixed in. This mixture was injected subcutaneously into the mammary fat pad of lightly anesthetized animals using a 27 gauge, 1/2 in. needle, after which animals were left to rest until tumors reached a palpable volume of 100 mm^3. Median tumor volume was around 140 mm^3, and animals that showed any physical characteristics of poor health (such as weight loss) or had dormant tumors lacking continuous growth were excluded from the study.

(c) *In Vivo* Administration. Once the tumor mass reached a palpable size of 100 mm^3, mice were randomly assigned to treatment with either PTX + CER in polymer-blend nanoparticles or PTX + CER as free drug (aqueous solution obtained by diluting the drugs from Cremophore EL:ethanol mixture), subdivided into groups of four mice per time point for a total of four time points (30 min, 1 h, 6 h, 12 h) per treatment group per tumor type. Each tumor bearing animal received a single dose intravenous injection (through the tail vein) of nanoparticle or free drugs at 1 μCi of PTX, and 0.5 μCi of CER diluted in sterile saline at an injection volume of 500 μL. At the conclusion of the biodistribution time points, mice were euthanized by CO_2 inhalation. Blood was collected by cardiac puncture, after which *in vivo* drug distribution was rapidly imaged by tracking the fluorescent output of rhodamine-PTX using a 565/690 nm filter set on a Kodak *In Vivo* FX Imaging Station (Rochester, NY).

(d) Radioactivity Analysis. Following this, blood, tumor, liver, spleen, kidney, lung, and heart were harvested and collected into preweighed test tubes. Tissue samples were homogenized at 10% (w/v) concentration in deionized distilled water, and 100 μL of tissue homogenate or blood was added into scintillation vials. Each sample was then digested in 1.0 mL of Scintigest tissue solubilizer (Thermo Fisher Scientific, Waltham, MA) at 55 °C for 2 h, followed by the addition of 200 μL of 30% (v/v) hydrogen peroxide (Thermo Fisher Scientific, Waltham, MA). This preparation was further incubated at 55 °C for 30 min, after which each sample received 10 mL of ScintiVerse scintillation fluid cocktail (Thermo Fisher Scientific, Waltham, MA). The samples were further left to quench in the dark for at least 2 h, after which counts of ^3H and ^{14}C were measured on an α/β scintillation counter. Scintillation counting for the free drug and nanoparticle doses administered was performed simultaneously to minimize variability. The results were expressed as percent of administered dose per gram of tissue or percent of administered dose per mL of blood.

Tumor and blood pharmacokinetic results were analyzed according to a noncompartmental pharmacokinetic model to determine mean retention time (MRT), half-life ($T_{1/2}$), volume of distribution (V_d), total body clearance (Cl_t), elimination rate constant (K), and area under the curve (AUC) for PTX and CER in tumor and blood.

4. Data Analysis. For drug biodistribution and pharmacokinetic profiling studies, $n = 4$ mice/group/time point. Statistical analysis was performed by using a two-tailed, Student's t test assuming equal variance in groups. We concluded that the differences were statistically significant at $p < 0.05$.

Results

Although earlier work[6] revealed the potency of a PTX + CER combination therapy to treat MDR ovarian cancer, it was observed that an important and interesting relationship existed within the kinetics of dosing PTX and CER. Figure 1 shows intracellular delivery of NBD-labeled CER using PLGA 70%/PbAE 30% blend nanoparticles in MCF7 and $MCF7_{TR}$ cells and verifies that cell-kill efficacy increased significantly when CER was administered with a delay of several hours following PTX administration in $MCF7_{TR}$ cells (Figure 1b), increasing from 39.1% cell death when the drugs were coadministered to 52.9% cell death when CER was administered 6 h following CER ($p < 0.05$). Interestingly, this increase was not observed when PTX was administered with a 6 h delay following CER (38.8% cell death) in this cell line. Additionally, the enhancement of cell-kill with CER coadministration was not observed in MCF7 (drug sensitive)

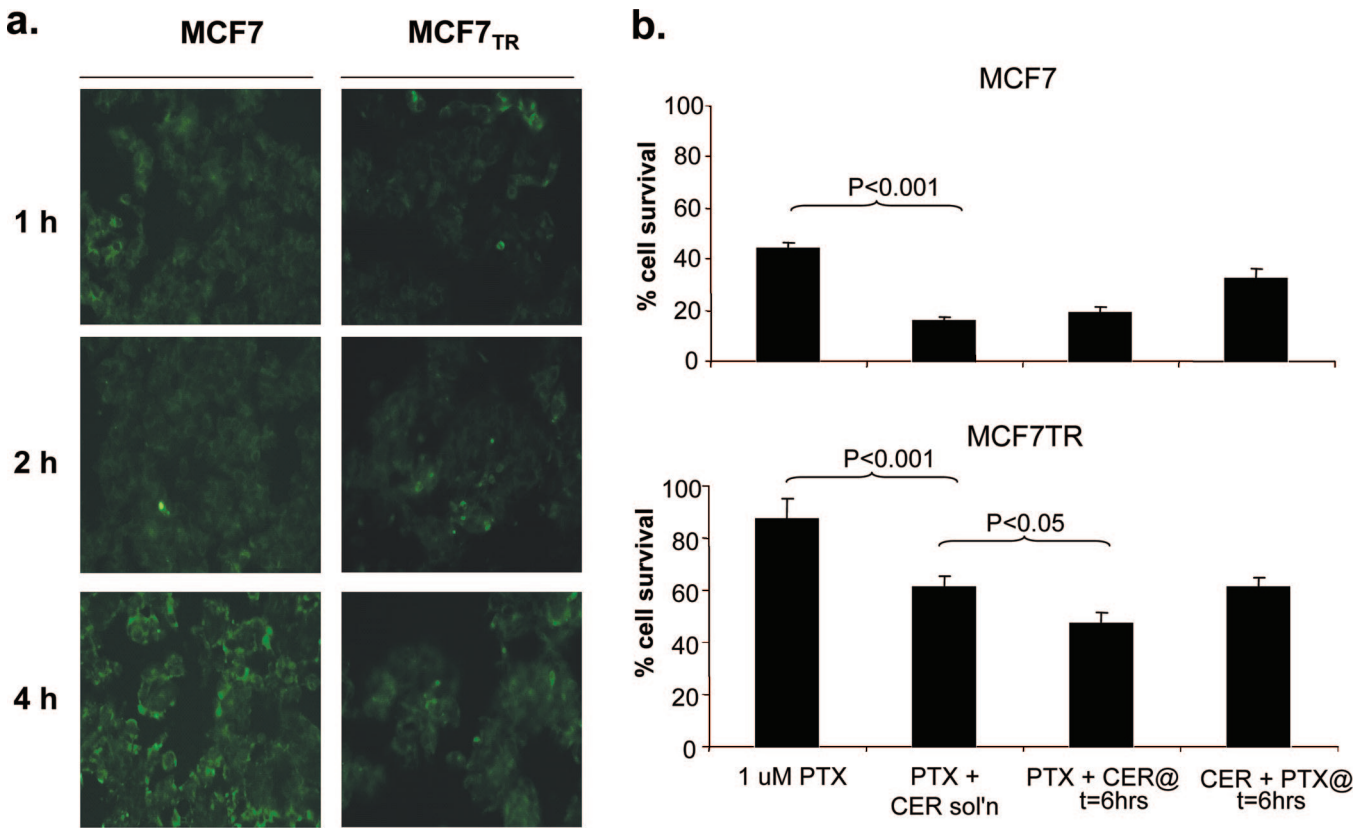

Figure 1. (a) Fluorescence microscopic evaluation of NBD-labeled C_6-ceramide (CER) delivery in MCF7 (drug sensitive) and $MCF7_{TR}$ (drug resistant) human breast adenocarcinoma cells. (b) Cell-kill efficacy of kinetic dosing between paclitaxel (PTX) and CER in MCF7 and $MCF7_{TR}$ cells when PTX was administered at $t = 0$, with CER administration at $t = 6$ h, or when CER is administered at $t = 0$, with PTX administration at $t = 6$ h ($n = 8$ samples/treatment).

cells as well. To incorporate this dose−kinetic relationship into the formulation, a nanoparticle system was designed that could simultaneously carry both the PTX and CER therapeutics, but release each in a controlled manner within the tumor cells. To achieve this temporally controlled release, PLGA was blended with a pH-responsive polymer, PbAE, at a ratio of 70% to 30% respectively. Table 1 summarizes the characterization of these particles. The particles were found to have an average size around 200 nm and a negative surface charge expected for the PLGA matrix. PTX and CER were loaded into the particles at 2.5% (w/w) for PTX and 10% (w/w) for CER to ensure preservation of the molar dosing ratio examined in *in vitro* studies (Figure 1) without compromising particle size or stability. At this load, loading yield was 100% for both drugs as determined by quantitative analysis of PTX and CER. The intention of this formulation was for PTX specifically to be localized with PbAE for immediate pH-responsive release upon internalization of the nanoparticles in the acidic tumor environment (pH 6.5). CER then was intended to incorporate within the PLGA regions of the nanoparticle for a slower, more sustained release, unaffected by the drop in pH at the tumor site. Thereby, the rapid release of PTX and the slower release of CER would impart the temporal controlled release profile that results in enhanced efficacy against MDR cancer. *In vitro* release simulations (Table 1) revealed just that: PTX experienced a surge in release upon a drop in pH to 6.5, while CER release remained unaffected when the pH decreased from 7.4 (physiological) to 6.5 (tumor). When the nanoparticles were incubated in PBS at pH 7.4, a similar amount of PTX and CER was relased in a one hour span (10.3% PTX and 12.3% CER). However, when the pH on the nanoparticles was dropped to 6.5 to mimic internalization into the tumor

Table 1. Characterization of the 70% PLGA/30% PbAE Polymer-Blend Nanoparticles for Physical Attributes, Drug Load, and Drug Release

Physical Characterization	
size (nm)	208.2 ± 5.7
zeta potential (mV)	−26.9 ± 5.4

Drug Encapsulation Efficacy		
	% entrapment	% yield
paclitaxel	2.5	100
C6-ceramide	10	100

In Vitro Drug Release (% Release in 1 h)		
	pH 7.4	pH 6.5
paclitaxel	10.3 ± 0.3	31.9 ±1.0
C6-ceramide	12.3 ± 1.7	7.6 ±1.3

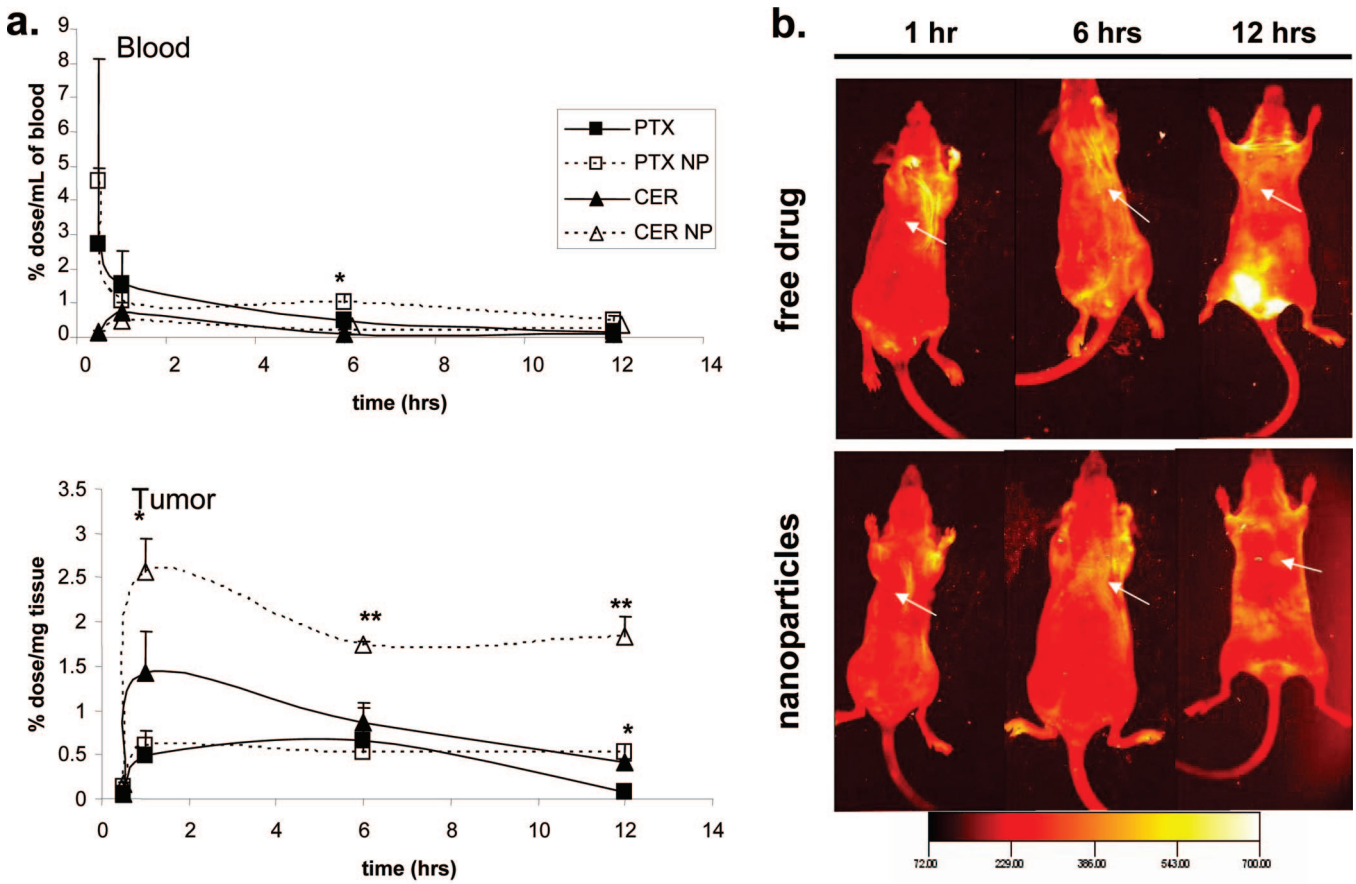

Figure 2. (a) Quantitative blood and tumor and (b) qualitative tumor biodistribution and pharmacokinetic profile of paclitaxel (PTX) and C_6-ceramide (CER) administered intravenously as free drug and upon encapsulation in poly(ethylene oxide)-surface modified poly(D,L-lactic-*co*-glycolic acid)/poly(beta-amino ester) [70:30% (w/w)] polymer-blend nanoparticle (NP) at 1, 6, and 12 h after administration to MCF7 (drug sensitive) tumor bearing mice. The symbols * and ** indicate statistical significance ($p < 0.05$ and $p < 0.001$, respectively) between NP and free drug treatment of each drug ($n = 4$ samples/group). The arrows indicate the tumor site as located on photographic images.

environment, PTX exhibited a surge of release (31.9% in 1 h) while the rate of CER release remained unchanged (7.6% in 1 h). These results verify that PTX release preceded that of CER by this pH-responsive trigger. With this formulation intact now, the effects on PTX and CER pharmacokinetics and biodistribution were examined.

To achieve a direct comparison between PTX and CER drug biodistribution and pharmacokinetics when administered as a conventional Cremophore EL-ethanol formulation versus encapsulation within the 70% PLGA/30% PbAE polymer-blend nanoparticles, both preparations were spiked with radiolabeled derivatives of PTX and CER. Both ^{3}H-PTX and ^{14}C-CER were encapsulated within the nanoparticle and free drug formulations as described in Materials and Methods in such a way that each animal received a tracer of 1.0 μCi of PTX and 0.5 μCi of CER of which the counts could be simultaneously read on an α/β- scintillation counter. Furthermore, to qualitatively assess drug biodistribution, and particularly tumor localization, resulting from the dose formulation, both the free drug and nanoparticle forms of drug were additionally spiked with a red-fluorescent derivative of PTX (rhodamine-PTX), which could be visualized *in vivo* using an *in vivo* imaging module.

Quantitative data was obtained by standardizing ^{3}H and ^{14}C cpm from individual tissues or blood by the counts-per-minute (cpm) for the dose administered per gram of tissue or mL of blood, to express tissue and blood drug levels over time as % of dose/g or mL. Figure 2a depicts the blood and tumor pharmacokinetic curves for both PTX and CER resulting from administration as free drug as compared to PbAE/PLGA blend nanoparticle delivery in mice bearing MCF7 drug sensitive orthotopic tumor xenografts. As expected, the data shows that nanoparticle delivery prolongs plasma retention of PTX over free drug administration, indicated by a 2-fold increase in PTX from nanoparticle delivery over free drug (1.02 ± 0.25 versus 0.46 ± 0.08% dose/mL respectively, $p < 0.05$). Similarly, tumor retention of PTX increases significantly with nanoparticle delivery of the drug, whereby at 12 h out 6.5-fold more PTX resides in the tumor mass compared with the free drug administration (0.53 ± 0.08 versus 0.08 ± 0.02%/g of nanoparticle versus free PTX, $p < 0.001$). What is more striking is that while

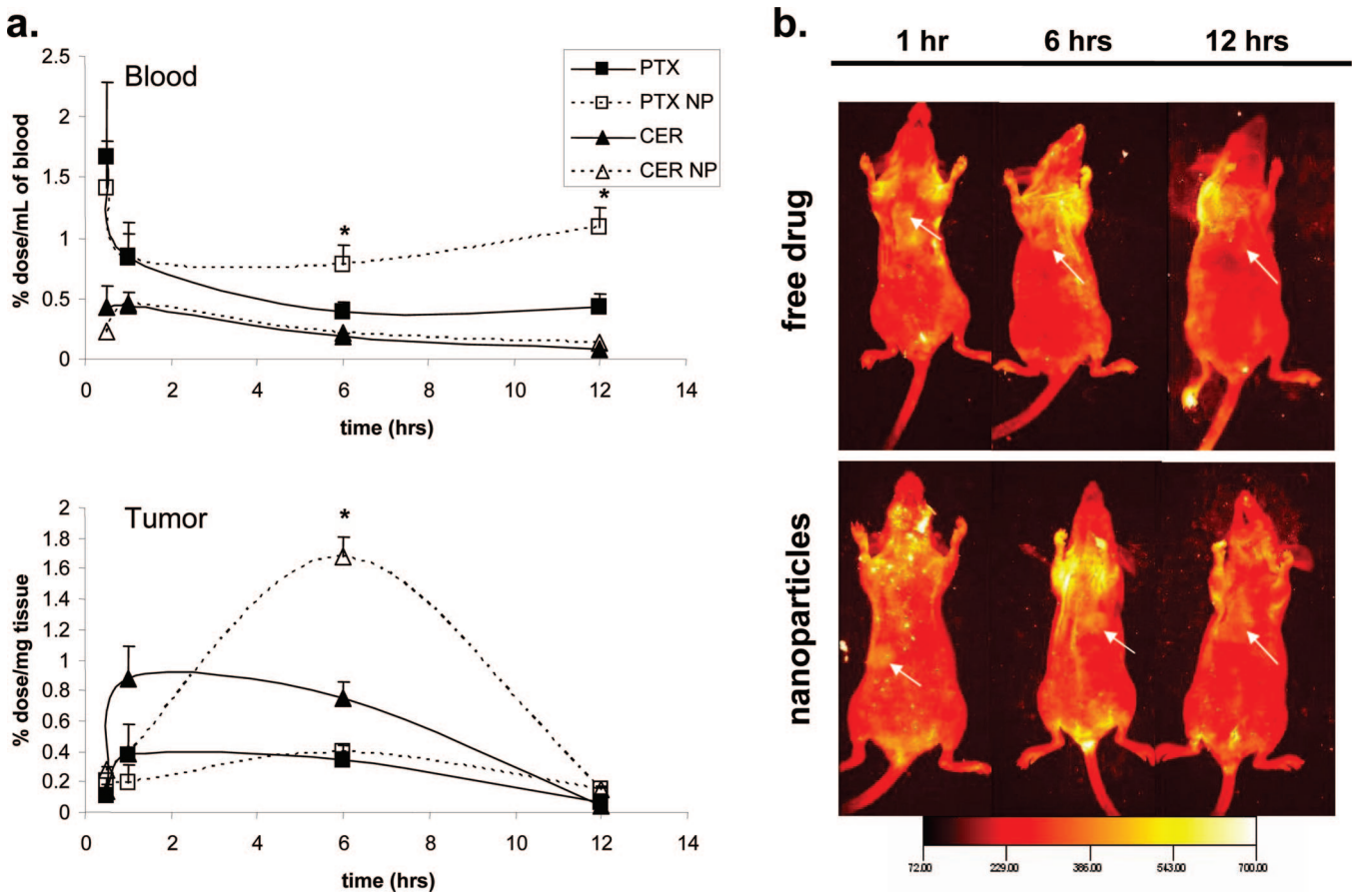

Figure 3. (a) Quantitative blood and tumor and (b) qualitative tumor biodistribution and pharmacokinetic profile of paclitaxel (PTX) and C_6-ceramide (CER) administered intravenously as free drug and upon encapsulation in poly(ethylene oxide)-surface modified poly(D,L-lactic-*co*-glycolic acid)/poly(beta-amino ester) [70:30% (w/w)] polymer-blend nanoparticle (NP) at 1, 6, and 12 h after administration $MCF7_{TR}$ (MDR) tumor bearing mice. The symbol ** indicates statistical significance ($p < 0.001$) between NP and free drug treatment of each drug ($n = 4$ samples/group). The arrows indicate the tumor site as located on photographic images.

nanoparticles did not affect CER retention in the blood significantly, the nanoparticles cause significant CER accumulation at the tumor site, initially a 2-fold increase early on at 1 and 6 h, elevating to a 4.5-fold increase by 12 h. Additionally, the maximal concentration of drug at the tumor site within this therapeutic window reaches a significantly higher peak with nanoparticle delivery over the free drug formulation (2.6 ± 0.4 versus 1.42 ± 0.5), a phenomenon that perhaps explains the efficacy seen with CER treatment alone. Qualitative biodistribution images that traced red-fluorescent PTX (Figure 2b) similarly revealed that while drug accumulation can be observed in tumors of mice subjected to free drug treatment 6 h out, this signal is lost by 12 h. However, the mice subjected to nanoparticle treatment retain their tumor accumulation signal beyond 6 h to retain visibility even at 12 h out. This result further suggests that the nanoparticles are retained for prolonged periods of time in the tumor mass.

Similar results were seen in the blood and tumor pharmacokinetic profiles of PTX and CER when administered to $MCF7_{TR}$ tumor bearing mice (Figure 3a). While nanoparticle delivery had no effect on blood retention of CER over free drug administration, PTX retention in the blood resulting from nanoparticle delivery elevated significantly 2- to 2.5-fold over that of free drug, for example to reach levels of 1.08 ± 0.16 versus 0.43 ± 0.11%/mL at 12 h from nanoparticle versus free drug administration respectively. Similar to the trend seen in the drug sensitive MCF7 tumor bearing mice, nanoparticles elevated not only PTX accumulation in the tumor mass 2-fold (0.15 ± 0.01 versus. 0.07 ± 0.00 at 12 h, $p < 0.001$), but particularly CER accumulation and maximal concentration (1.7 ± 0.13 versus 0.75 ± 0.1 at 6 h, $p < 0.001$). Figure 3b depicts qualitative biodistribution images for the $MCF7_{TR}$ tumor bearing mice that once more revealed that while drug accumulation can be observed in tumors of mice administered free drug 6 h out, this signal is lost by 12 h, while the mice subjected to nanoparticle treatment retain their tumor accumulation signal at both 6 and 12 h out.

Analysis of tumor and blood pharmacokinetic data by noncompartmental pharmacokinetics revealed how nanoparticle drug delivery altered key pharmacokinetic parameters for both PTX and CER. Table 2 and Table 3 summarize the pharmacokinetic parameters of PTX and CER from free drug administration and nanoparticle delivery in blood (plasma) and tumor respectively. As suggested by the plots in Figure

Table 2. Summary of Plasma Noncompartmental Pharmacokinetic Parameters of Paclitaxel (PTX) and Ceramide (CER) Resulting from Administration as Free Drug as Compared to Delivery in PLGA/PbAE Polymer-Blend Nanoparticles[a]

pharmacokinetic parameter	PTX	PTX nanoparticle	CER	CER nanoparticle
MCF7:				
AUC (% dose·h/mL)	6.9 ± 1.7	10.5 ± 2.1	2.5 ± 0.8	2.9 ± 0.4
MRT (h)	23.9 ± 10.7	25.1 ± 9.3	347.7 ± 107.5	1470 ± 483
K (h^{-1})	0.07 ± 0.02	0.05 ± 0.01	0.003 ± 0.001	0.0009 ± 0.0006
$T_{1/2}$ (h)	16.6 ± 7.4	17.4 ± 6.4	240.9 ± 75.5	1019 ± 335.1
Cl_t (% dose·h/(% dose/mL))	0.009 ± 0.002	0.005 ± 0.001	0.12 ± 0.04	0.07 ± 0.01
V_d (% dose/(% dose/mL))	0.22 ± 0.10	0.14 ± 0.07	36.6 ± 20.7	130.4 ± 48.8
$MCF7_{TR}$:				
AUC (% dose·h/mL)	5.2 ± 0.9	10.2 ± 0.9*	2.27 ± 0.3	2.9 ± 0.1
MRT (h)	115.4 ± 43.3	54.0 ± 19.6	166.7 ± 90.1	182.5 ± 25.1
K (h^{-1})	0.007 ± 0.004	0.020 ± 0.007	0.007 ± 0.005	0.004 ± 0.001
$T_{1/2}$ (h)	80.0 ± 30.0	37.4 ± 13.6	115.5 ± 62.5	126.5 ± 17.4
Cl_t (% dose·h/(% dose/mL))	0.010 ± 0.001	0.005 ± 0.000*	0.09 ± 0.01	0.07 ± 0.00
V_d (% dose/(% dose/mL))	1.4 ± 0.6	0.25 ± 0.06	17.8 ± 11.2	12.8 ± 1.8

[a] AUC = area under the curve; MRT = mean residence time; K = elimination rate constant; $T_{1/2}$ = half-life; Cl_t = total body clearance; V_d = volume of distribution. The symbols * indicate statistical significance ($p < 0.05$) between free drug and nanoparticle dosage forms for each drug at the given pharmacokinetic parameter ($n = 3-4$ repeats/group).

Table 3. Summary of Tumor Noncompartmental Pharmacokinetic Parameters of Paclitaxel (PTX) and Ceramide (CER) Resulting from Administration as Free Drug as Compared to Delivery in PLGA/PbAE Polymer-Blend Nanoparticles[a]

pharmacokinetic parameter	PTX	PTX nanoparticle	CER	CER nanoparticle
MCF7:				
AUC (% dose·h/g)	4.9 ± 2.3	6.0 ± 1.0	9.0 ± 0.9	22.5 ± 0.9**
MRT (h)	114.7 ± 53.0	308.4 ± 119.0	39.0 ± 13.8	43.9 ± 6.7
K (h^{-1})	0.011 ± 0.005	0.005 ± 0.002	0.04 ± 0.02	0.024 ± 0.004
$T_{1/2}$ (h)	79.5 ± 36.7	213.7 ± 82.5	27.0 ± 9.5	30.4 ± 4.7
Cl_t (% dose·h/(% dose/g))	0.017 ± 0.006	0.009 ± 0.001	0.023 ± 0.003	0.008 ± 0.000*
V_d (% dose/(% dose/g))	3.7 ± 1.6	2.9 ± 1.2	0.9 ± 0.3	0.39 ± 0.07
$MCF7_{TR}$:				
AUC (% dose·h/g)	2.9 ± 0.6	3.2 ± 0.5	6.47 ± 0.5	11.0 ± 0.9**
MRT (h)	81.7 ± 67.9	153.0 ± 117.8	5.9 ± 0.4	6.5 ± 0.2
K (h^{-1})	0.05 ± 0.02	0.02 ± 0.01	0.17 ± 0.01	0.15 ± 0.00
$T_{1/2}$ (h)	56.6 ± 47.0	106.0 ± 81.6	4.1 ± 0.2	4.5 ± 0.1
Cl_t (% dose·h/(% dose/g))	0.019 ± 0.004	0.02 ± 0.002	0.031 ± 0.002	0.018 ± 0.001**
V_d (% dose/(% dose/g))	2.19 ± 2	3.1 ± 2.5	0.19 ± 0.03	0.12 ± 0.01

[a] AUC = area under the curve; MRT = mean residence time; K = elimination rate constant; $T_{1/2}$ = half-life; Cl_t = total body clearance; V_d = volume of distribution. The symbols * and ** indicate statistical significance ($p < 0.05$ and $p < 0.001$, respectively) between free drug and nanoparticle dosage forms for each drug at the given pharmacokinetic parameter ($n = 3-4$ repeats/group).

2 and Figure 3, nanoparticle delivery increased area-under-the-curve (AUC) in blood, for PTX but not for CER (Table 2). While mean retention time (MRT), the elimination constant (K), half-life ($T_{1/2}$) and volume of distribution (V_d) appeared unchanged for either drug between free drug administration and nanoparticle delivery in the blood, nanoparticles did significantly lower the rate of total body clearance (Cl_t) for PTX, albeit not for CER, thereby supporting the idea that nanoparticles promote prolonged PTX retention in the blood. Oppositely, though, nanoparticles promoted a significantly increased AUC and decreased Cl_t for CER in the tumor tissue (Table 3), although at this site pharmacokinetics of PTX remained unchanged between nanoparticle versus free drug delivery. Interestingly, though, it can be concluded from this study that nanoparticle delivery does benefit both drug treatments, by increasing PTX levels and prolonging PTX retention in the circulation, and by increasing CER retention and decreasing CER clearance from the tumor site.

Lastly, to determine the effects of nanoparticle delivery of PTX and CER compared with administration of free PTX and CER on nontarget distribution, drug distribution over time was monitored in liver, kidney, spleen, lung, and heart, as illustrated in Figure 4 for MCF7 tumor bearing mice, and Figure 5 for $MCF7_{TR}$ tumor bearing mice. From this data, it appears that while nanoparticle delivery does not significantly alter peak concentrations of PTX or CER that accumulate the examined nontarget organs, nanoparticle delivery does appear to prolong clearance of either drug from these nontarget organs. At 6 h postadministration, similar amounts of PTX and CER could be detected in the liver, kidney, spleen, lung and heart of mice bearing either drug sensitive or MDR tumor types. Twelve hours postadministration, traces of both PTX and CER are nearly undetectable in the liver,

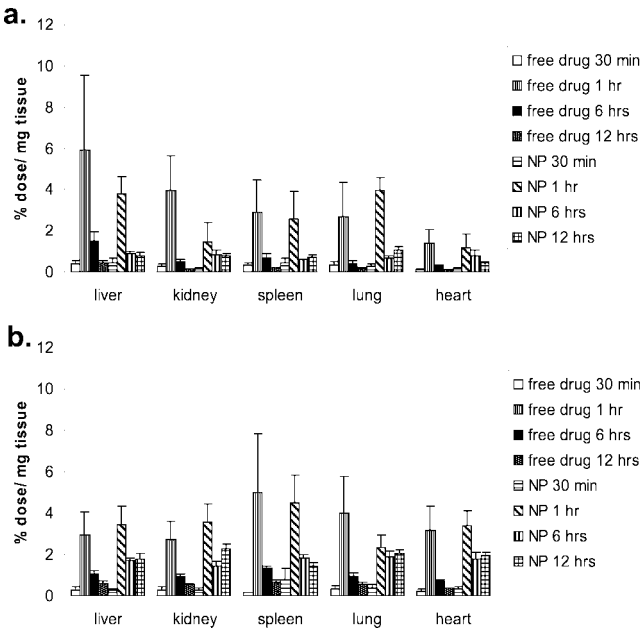

Figure 4. Quantitative tissue biodistribution profile of (a) paclitaxel (PTX) and (b) C_6-ceramide (CER) administered as free drug or in poly(ethylene oxide)-surface modified poly(D,L-lactic-*co*-glycolic acid)/poly(beta-amino ester) [70: 30% (w/w)) polymer-blend nanoparticle formulations at 1, 6, and 12 h after intravenous administration in MCF7 (drug sensitive) tumor bearing mice.

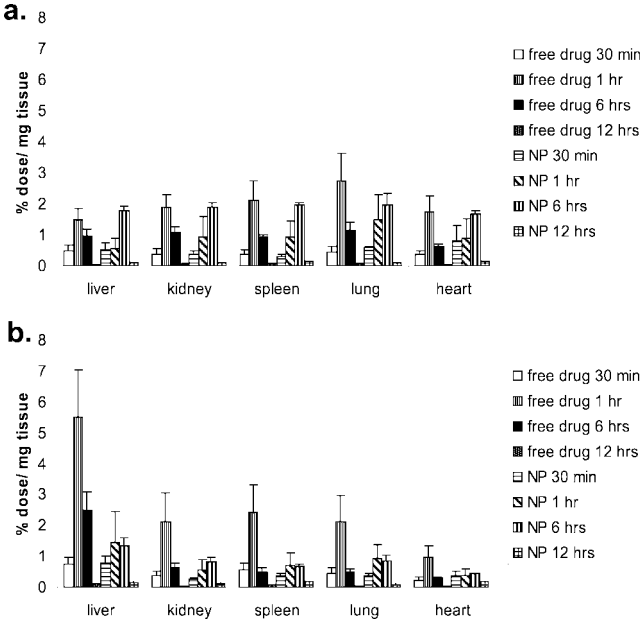

Figure 5. Quantitative tissue biodistribution profile of (a) paclitaxel (PTX) and (b) C_6-ceramide (CER) administered as free drug or in poly(ethylene oxide)-surface modified poly(D,L-lactic-*co*-glycolic acid)/poly(beta-amino ester) [70: 30% (w/w)) polymer-blend nanoparticle formulations at 1, 6, and 12 h after intravenous administration in $MCF7_{TR}$ (drug resistant) tumor bearing mice.

kidney, spleen, lung and heart of these mice, suggesting clearance of the majority of the administered drug. However, nanoparticle delivery of both PTX and CER are retained at a significantly higher level in these tissue types by 12 h postadministration. Curiously, though, this effect is only observed in mice bearing the MCF7 tumor type, while no differences exist between nanoparticle and free drug retention at 12 h for the $MCF7_{TR}$ tumor bearing mice. Although a prolonged retention at nontarget tissues could be a factor for toxicity, extensive studies examining white blood cell counts and liver enzyme activity following both acute and chronic administration of this nanoparticle therapy revealed that the therapy was well tolerated since no such toxicity arises (data not shown).

Discussion

It is widely known that nanoparticles are beneficial tumor targeting vehicles due to their passive targeting properties by the enhanced permeability and retention (EPR) effect, whereby the added advantage of stealth shielding the particles with a poly(ethylene glycol/oxide) (PEO/PEG) surface modification avoids uptake by the reticuloendothelial system, thereby improving circulation time of the nanoparticles.[22] The formulation described herein is for a blend of slow releasing PLGA and pH-responsive rapid releasing PbAE for temporal controlled release of PTX with CER to treat MDR cancer, whereby the nanoparticle was surfaced modified with PEO to promote stealth shielding and prolonged circulation of the combination drug therapy. Using radiolabeled derivatives of PTX and CER, namely ^{3}H-PTX and ^{14}C-CER, it was possible to quantitatively track drug distribution over time *in vivo* resulting from administration as free drug versus encapsulation within the polymer-blend nanoparticles.

Drug distribution was monitored in mice bearing either drug sensitive MCF7 or MDR $MCF7_{TR}$ tumors, since differences between the physiology of these two tumor types could potentially lead to differences in drug disposition and retention at the tumor site specifically. Surprisingly, there was no difference in magnitude between the tumor accumulations at 6 h after administration of free PTX, nanoparticle PTX, free CER, or nanoparticle CER between the drug sensitive and MDR tumors. Beyond 6 h, levels of PTX and CER delivered by nanoparticles remained unchanged in the MCF7 tumors, while levels of PTX and CER delivered as free drug began to decrease. Overall, the amount of tumor accumulation of both drugs administered in nanoparticles significantly exceeded that of free drug administration at some of the tested time points in the MCF7 tumor bearing animals. This finding supports the hypothesis of enhanced tumor accumulation and retention of nanoparticle-delivered drugs by the EPR effect.[20] However, the effects seen in the MDR $MCF7_{TR}$ tumors were very different. While the magnitude of drug accumulation between the two tumor types was no different, intratumoral levels of PTX and CER from both free drug and nanoparticle administration tumors dropped drastically in the $MCF7_{TR}$ after 6 h to nearly entirely disappear from the tumor by 12 h after administra-

(22) Gref, R.; Minamitake, Y.; Peracchia, M. T.; Trubetskoy, V.; Torchilin, V.; Langer, R. *Science* **1994**, *263* (5153), 1600–1603.

tion, whereas drug levels remained steady during this period in the MCF7 tumors. This finding suggests that drug efflux pumps like P-glycoprotein mediate removal of both PTX and CER from the MDR tumor after 6 h, although, since only free drug is susceptible to efflux, we cannot conclude that the drugs must have been released from the nanoparticles by this time point. Although the amount of nanoparticle-delivered CER reaching $MCF7_{TR}$ tumors exceeded the amount of CER administered as free drug by 2-fold, similar to the results seen in the MCF7 tumors, we did not observe this increase in PTX delivered as free drug versus nanoparticles. However, this result is in accordance with the prediction that the bulk of PTX releases immediately from this nanoparticle upon internalization into the tumor environment from a drop in pH. Unfortunately, the presence of P-glycoprotein efflux pumps appears to quickly remove the released PTX from the tumor site. Nevertheless, the results still support the increased tumor accumulation of nanoparticle delivered drugs by the EPR effect in the $MCF7_{TR}$ tumors as well, although retention of the drugs in the tumor site is hindered by the P-glycoprotein mediated efflux. The systemic pharmacokinetic parameters of CER administered as free drug or nanoparticles were very similar in magnitude and profile between MCF7 and $MCF7_{TR}$ tumor bearing mice. Interestingly, in both animal models, plasma CER does not display a profile characteristic of instantaneous input. Rather, CER blood pharmacokinetics exhibit profiles that are more representative of oral absorption. Although the hydrophobicity of free CER may lead to longer residence times at the site of injection, nanoparticle formulations of CER behave similarly while not exhibiting such hydrophobicity. It is unlikely that CER is prematurely released from the nanoparticle to linger at the injection site, since tumor pharmacokinetic results imply that CER is retained in the nanoparticle by 6 h after administration. Since tumor and nonspecific target accumulation of CER follows a similar profile as PTX, with peak accumulation at 1 h after administration (with the exception of $MCF7_{TR}$ tumors, where peak accumulation occurred at 6 h), it is again unlikely that peak CER plasma levels take place prior to 30 min after administration. Unfortunately, the pharmacokinetics of CER and other sphingolipids following intravenous administration have not been evaluated to date by other groups, forbidding conclusive statements regarding plasma CER pharmacokinetics. Thus, at this point, it can merely be speculated that CER perhaps resides on the surface of the nanoparticle rather than internally to behave more like free CER in the circulation. This could cause CER of either formulation to linger at the injection site or sequester in more lipophilic compartments.

Systemic pharmacokinetics of PTX, on the other hand, behaved similarly to the pharmacokinetic profile obtained in other studies,[16] and displayed a profile characteristic of instantaneous input whereby peak concentration occurred at the time of injection, with a subsequent disappearance of PTX from the plasma over time. In both the MCF7 and $MCF7_{TR}$ tumor bearing mice, PTX administration as free drug peaked upon administration, with a gradual decrease over time to culminate at nearly undetectable levels by 12 h after administration. Nanoparticle administration, on the other hand, caused a prolonged retention of PTX in the circulation of both MCF7 and $MCF7_{TR}$ tumor bearing mice seen by the increased amount of drug present in the circulation at 6 h after administration, compared to the amount of free drug present at this time point. Although it appears that PTX retention is more prominent in the $MCF7_{TR}$ tumor bearing mice over MCF7 tumor bearing mice, the magnitude of plasma drug level between these two animal models is very similar throughout all time points. These results are supportive of the known effects of PEO-surface modification on nanoparticles to produce prolonged circulation by stealth shielding, and agree well with the blood and tumor pharmacokinetic profile determined for PTX from free drug administration and nanoparticle delivery in SKOV3 tumor bearing mice.[15]

An evaluation of nonspecific target accumulation revealed that PTX administration in nanoparticles did not significantly alter nontarget accumulation over that of free drug, with neither an increase nor a decrease in drug retention in the most perfused tissues. This result is identical to similar studies conducted for nanoparticle versus free drug accumulation of PTX at nonspecific sites.[23] Although other studies have reported a decreased accumulation in liver, spleen, and lung resulting from nanoparticle administration,[24] we did not observe such results. On the other hand, although CER does not accumulate to any greater amount in nontarget tissues between free drug and nanoparticle administration, the nanoparticle dosage form does result in a prolonged retention of CER in all five nontarget tissues examined, liver, kidney, spleen, lung, and heart. It should be noted that this result was only seen in the MCF7 tumor bearing mice, while not in the $MCF7_{TR}$ tumor bearing mice. Given this inconsistency, it is uncertain whether CER truly is retained in nonspecific tissues for a prolonged period of time, since it is unlikely that the physiological differences between tumors would affect nontarget drug disposition.

Nevertheless, not only do the results demonstrate that nanoparticle delivery enhances tumor accumulation of drugs, supporting the well-known characteristic of nanoparticle tumor targeting by the EPR effect, but more importantly, the results demonstrate the effect that MDR tumor physiology may have on drug disposition at the target site despite EPR targeting. This knowledge could help factor into the design of nanoparticle platforms to enhance tumor targeting even in the presence of physiological barriers such as the presence of P-glycoprotein.

Conclusions

Long-circulating PEO-modified nanoparticles have been shown to accumulate preferentially in the solid tumor upon

(23) Zhang, C.; Qu, G.; Sun, Y.; Wu, X.; Yao, Z.; Guo, Q.; Ding, Q.; Yuan, S.; Shen, Z.; Ping, Q.; Zhou, H. *Biomaterials* **2008**, *29* (9), 1233–1241.

(24) Yang, T.; Cui, F. D.; Choi, M. K.; Cho, J. W.; Chung, S. J.; Shim, C. K.; Kim, D. D. *Int. J. Pharm.* **2007**, *338* (1−2), 317–326.

systemic administration. In this study, we have examined the delivery of combination PTX and CER to modulate the apoptotic threshold in tumor MDR by formulating both of these drugs in a single PLGA/PbAE (70:30 by weight) blend nanoparticles. When administered in an orthotopic (drug sensitive) MCF7 and multidrug resistant $MCF7_{TR}$ human breast adenocarcinoma model established in the mammary pad of female *nu/nu* mice, the nanoparticle-mediated delivery enhanced circulating times *in vivo* and allowed passive targeting to the tumor mass. The pharmacokinetic analysis revealed a trend for nanoparticle-mediated delivery of PTX toward the reduced clearance of the drug from the systemic circulation and tumor mass. We anticipate that the decreased PTX clearance would have significant implication in the treatment of MDR tumors. Overall, these results are encouraging for the development of multifunctional nanoparticle systems that can deliver combination therapy for synergistic effects, especially in refractory diseases.

Acknowledgment. This study was supported by the Nanotechnology Platform Partnership grant (R01-CA119617) from the National Cancer Institute (NCI) of the U.S. National Institutes of Health. L.E.V. is a recipient of a NCI and National Science Foundation (NSF) Interdisciplinary Graduate Education and Training (IGERT) predoctoral fellowship in Nanomedical Science and Technology.

MP800030K